

Conference materials

UDC 538.9

DOI: <https://doi.org/10.18721/JPM.161.320>

Electrically controlled switching between spatially separated conducting channels in a quantum point contact

D.I. Sarypov^{1,2} ✉, D.A. Pokhabov^{1,2}, A.G. Pogosov^{1,2},
E.Yu. Zhdanov^{1,2}, A.K. Bakarov^{1,2}

¹Rzhanov Institute of Semiconductor Physics, Novosibirsk, Russia;

²Novosibirsk State University, Novosibirsk, Russia

✉ d.sarypov@g.nsu.ru

Abstract. We demonstrate transverse magnetic focusing of electrons in semiconductor devices consisting of two trenched-type quantum point contacts (QPC) acting as an injector and a detector. The peak in the detector voltage, corresponding to the penetration of injected electrons into the detector, is observed. Applying the voltage difference between injector side gates is found to cause an abrupt shift of the peak position on the magnetic field scale. This shift can be explained by switching between spatially separated channels inside the multi-well potential formed inside a QPC-injector.

Keywords: ballistic electron transport, quantum point contact, multichannelity, multi-well potential, transverse magnetic focusing

Funding: The study was funded by the Russian Science Foundation (project 22-12-00343 – experimental measurements) and the Ministry of Science and Higher Education of the Russian Federation (project FWGW-2022-0011 – characterization of initial heterostructures).

Citation: Sarypov D.I., Pokhabov D.A., Pogosov A.G., Zhdanov E.Yu., Bakarov A.K., Electrically controlled switching between spatially separated conducting channels in a quantum point contact. St. Petersburg State Polytechnical University Journal. Physics and Mathematics. 16 (1.3) (2023) 117–123. DOI: <https://doi.org/10.18721/JPM.161.320>

This is an open access article under the CC BY-NC 4.0 license (<https://creativecommons.org/licenses/by-nc/4.0/>)

Материалы конференции

УДК 538.9

DOI: <https://doi.org/10.18721/JPM.161.320>

Электрически контролируемое переключение между пространственно разделенными проводящими каналами в квантовом точечном контакте

Д.И. Сарыпов^{1,2} ✉, Д.А. Похабов^{1,2}, А.Г. Погосов^{1,2},
Е.Ю. Жданов^{1,2}, А.К. Бакаров^{1,2}

¹Институт физики полупроводников им. А.В. Ржанова Сибирского отделения РАН, г. Новосибирск, Россия;

²Новосибирский государственный университет, г. Новосибирск, Россия

✉ d.sarypov@g.nsu.ru

Аннотация. Исследована магнитная фокусировка электронов в полупроводниковых устройствах, состоящих из двух одинаковых КТК траншейного типа (инжектор и детектор). Наблюдается пик в напряжении детектора, соответствующий попаданию инжектированных электронов в детектор. Приложение разности напряжений между затворами инжектора приводит к резкому смещению фокусировочного пика, что может быть объяснено переключением между пространственно разделенными проводящими каналами в КТК инжекторе.

Ключевые слова: баллистический электронный транспорт, квантовый точечный контакт, многоканальность, многоямный потенциал, магнитная фокусировка

Финансирование: РФ (проект №22-12-00343 – экспериментальные измерения); Министерство науки и высшего образования РФ (проект №FWGW-2022-0011 – характеристика исходных гетероструктур).

Ссылка при цитировании: Сарыпов Д.И., Похабов Д.А., Погосов А.Г., Жданов Е.Ю., Бакаров А.К. Электрически контролируемое переключение между пространственно разделенными проводящими каналами в квантовом точечном контакте // Научно-технические ведомости СПбГПУ. Физико-математические науки. 2023. Т. 16. № 1.3. С. 117–123. DOI: <https://doi.org/10.18721/JPM.161.320>

Статья открытого доступа, распространяемая по лицензии CC BY-NC 4.0 (<https://creativecommons.org/licenses/by-nc/4.0/>)

Introduction

The conductance quantization in units of $2e^2/h$ [1, 2] is a hallmark of quasi-one-dimensional electron transport inherent in quantum point contacts (QPC) — point microconstriction in a two-dimensional electron gas (2DEG) with a width comparable to the Fermi wavelength of electrons. Nowadays a number of conductance quantization features lying beyond a single particle model remain unclear. In recent contributions a trenched-type QPC created by means of lithographic trenches separating the conducting area from two side gates is shown to experience an unusual effect of multichannelity [3–7]. The effect consists in the formation of several channels inside the QPC, which conductances are separately quantized and add up. The effect observation is promoted by the feature of a trenched-type QPC allowing to apply both positive and negative potentials to the gates, as well as large voltage differences between the gates [8] and investigate the QPC conductance in a wide range of the sum and difference of gate voltages.

The physical mechanism of multichannelity is supposed to be linked with a correlated redistribution of charges in the heterostructure (electrons of 2DEG and positively charged donors) caused by their Coulomb interaction leading to the formation of multi-well confining potential. The self-consistent numerical calculation presented in [7] describes the formation conditions of a multi-well confining potential. The creation of multi-well potential due to Coulomb interaction is shown in simulations performed in other articles dealing with a split-gate QPC [9] and bilayer graphene [10].

The conductance measurements described above allow obtaining only the implicit evidence of multichannelity. Therefore, transverse magnetic focusing (TMF) [11, 12] was chosen to investigate the multichannelity since it can be used to directly discern the channels existing in the QPC through the separation of its contribution to the measured signal on a magnetic field scale [13, 14].

In the present work we report on the investigation of the multichannel electron transport in the trench-type QPC by means of the TMF experiments. The devices consisting of two trench-type QPCs are created for this purpose. Each of the QPCs is supplied with two symmetric side gates. In the experiment one QPC acts as a monochromatic injector of ballistic electrons, another one plays a role of a point detector. The focusing peaks corresponding to the registration of injected electrons emerge in the detector voltage as a function of magnetic field. The cyclotron diameter of 4 "μm" corresponding to the magnetic field of "70 mT" at the top of the peak is shown to coincide with the injector-detector separation of 4 "μm". The application of gate voltage difference between side gates is found out to shift the focusing peak. The peak was shifted by 2 mT (by 3% of resonance magnetic field) which is the experimental evidence of conducting channel displacement in the QPC-injector at about 100 nm. This value is comparable with the characteristic distance between channels [4, 6]. Interestingly, the shift occurs abruptly, and that can be interpreted as switching between conducting channels inside the QPC-injector, which confining potential is multi-well.

Materials and Methods

Experimental samples are created from the GaAs/AlGaAs heterostructure grown by molecular beam epitaxy on a GaAs substrate (Fig. 1, *a*). It has a short-periodical AlAs/GaAs superlattice and a 13 nm GaAs layer located in the middle and acts as a symmetrical quantum well for electrons. Doping the heterostructure with Si δ -layers symmetrically relative to the quantum well allows electrons to fill it and form a 2DEG. A feature of the heterostructure used is that it contains low-mobility X-valley electrons localized on Si-donors, which characteristic concentration is $n_x \sim 10^{10} \text{ cm}^{-2}$. X-valley electrons do not give a contribution to the conductance but smooth the fluctuations of electrostatic potential of random impurities thereby increasing the 2DEG mobility [15]. The 2DEG density and mobility at $T = 4.2 \text{ K}$ are $n_{2D} = 7 \times 10^{11} \text{ cm}^{-2}$ and $\mu = 2 \times 10^6 \text{ cm}^2/(\text{V}\cdot\text{s})$, respectively. The presence of the $\text{Al}_{0.8}\text{Ga}_{0.2}\text{As}$ layer does not affect the observation of multichannelity. This layer can be used to create suspended (separated from the substrate) nanostructures [16, 17], but we study the non-suspended structure.

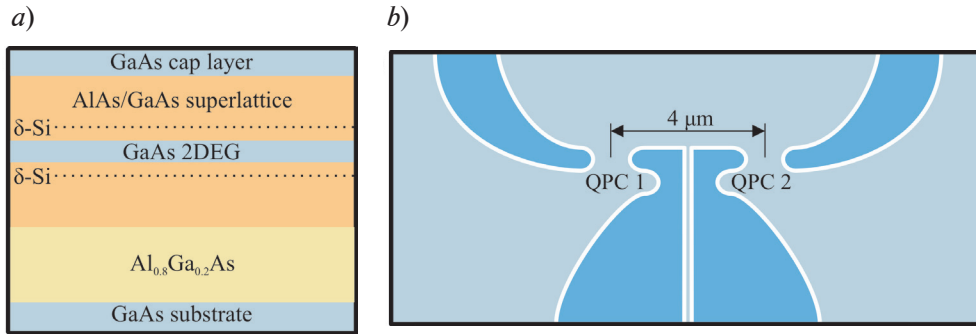


Fig. 1. Schematic images of the heterostructure with the 2DEG doped with Si δ -layers (*a*) and the experimental sample for transverse magnetic focusing (*b*). The lithographic trenches separating conducting area (lighter region) from the gates (darker regions) are marked in white

The devices for the TMF experiments consist of two parallel and similar trrenched-type QPCs (injector and detector) separated at the distance of $4 \mu\text{m}$ (less than mean free path length $l \approx 20 \mu\text{m}$) from each other in the direction perpendicular to the channel direction (Fig. 1, *b*). Both the QPC-injector and QPC-detector have adiabatic form optimal for the magnetic focusing [18]. The injector and detector have individual sources and common drains. The lithographic width of the QPC is about 900 nm and the curvature radius of side gates near the QPC is 500 nm. The electron injection was carried out by the ac source-drain bias with the magnitude of $100 \mu\text{V}$. The detector voltage was measured by means of the lock-in technique as a function of transverse magnetic field. All measurements were performed at $T = 1.6 \text{ K}$.

Results and Discussion

The relative detector voltage $[V(B) - V(0)]/V(0)$ as a function of transverse magnetic field at fixed injector and detector conductance ($G_{\text{inj}} = G_{\text{det}} = 2e^2/h$) is shown in Fig. 2. The potentials on the side gates remained symmetrical. The measurement configuration is shown in the inset to Fig. 2. A distinct peak is seen at the field $B^* \approx -70 \text{ mT}$. The cyclotron diameter corresponding to $B^* d_c = 2\hbar\sqrt{2\pi n_{2D}}/eB^* \approx 4 \mu\text{m}$ turns out to be equal to the distance between the injector and detector. Therefore, geometrical resonance relating to the injected electron ingress into the detector is observed at this field. The corresponding ballistic trajectory is shown with the arrow in the inset to Fig. 2. A similar peak is not observed at $B > 0$ since electrons at the positive magnetic field move in the direction opposite to the detector. Further we will consider only the range of the field containing the focusing peak. The inversion of the detector and the injector leads to the similar picture due to their symmetry.

A series of the detector voltage dependences on the magnetic field shown in Fig. 3, *a* is obtained by applying voltage difference ΔV_G to the injector gates. Each curve corresponds to the different value of ΔV_G . The curves are vertically shifted from each other for clarity. The voltage difference ΔV_G was changed in a wide range of values from -20 to $+20 \text{ V}$. The sum of gate voltages remained constant and equal $\Sigma V_G = -12 \text{ V}$. Range of the field containing the focusing peak is shown in Fig. 3, *b* where the detector voltage maxima are marked by circles. The peak position as a function

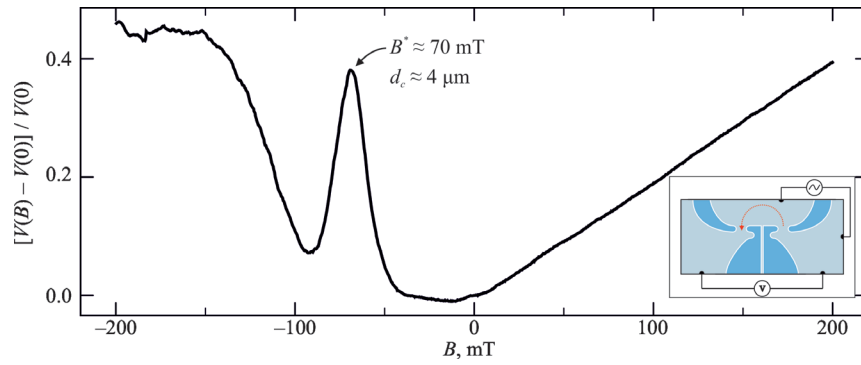


Fig. 2. Relative detector voltage as a function of the transverse magnetic field at symmetrical potentials on the side gates. The inset gives the measurement configuration. The trajectory at the resonance magnetic field is shown with the arrow

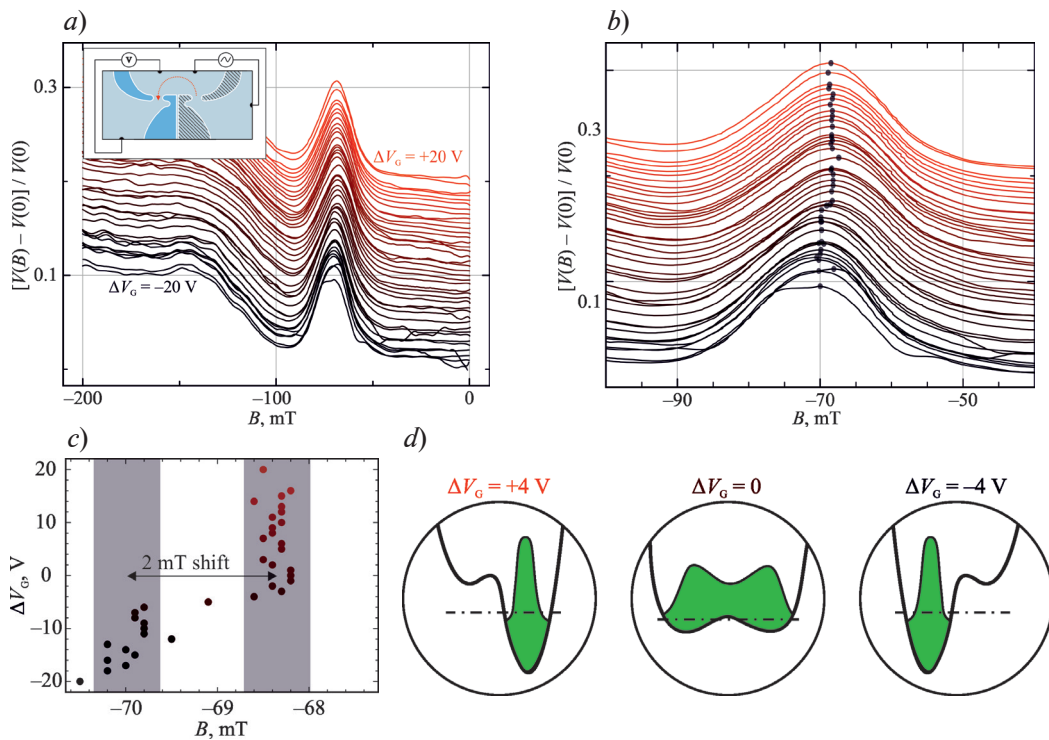


Fig. 3. Dependence of the detector voltage on the magnetic field at various ΔV_G of the injector (applied to dashed gates) changing from -20 to $+20$ V (a); the lower curve corresponds to -20 V, upper curve to $+20$ V. The sum of gate voltages was fixed ($\Sigma V_G = -12$ V). Measurement configuration is shown in the inset. The panel in (b) shows the dependence in (a) on an enlarged scale. The maxima of the detector voltage are marked by circles. Peak position as function of ΔV_G (c). Illustration of shift of the electron density in the injector when applying ΔV_G (d). Fermi energy is marked by a dash-dotted line

of ΔV_G is shown in Fig. 3, c. It is seen that, at $\Delta V_G < 0$ the focusing peaks are observed near $B_1 = -70$ mT, while at $\Delta V_G > 0$ they are concentrated near $B_2 = -68$ mT. Thus, we observe a abrupt shift of the focusing peak by $\Delta B \sim 2$ mT at $\Delta V_G \approx 0$. This rapid shift corresponds to the change of cyclotron diameter $\Delta d_c \sim 100$ nm (comparable with the characteristic distance between the channels determined from the analysis of the experimentally measured capacitance coefficients [4, 6]) that can be interpreted as an abrupt shift of the conducting channel inside the QPC-injector when the ΔV_G sign changes. The abrupt shift can be evidence of the formation of a double-well potential inside the QPC-injector. Applying the voltage difference to the gates gives an addition to the confining potential $\Delta U(x) = \alpha x$, linearly dependent on the coordinate x perpendicular to the channel in a 2DEG plane. If the potential was single-well, applying ΔV_G

would only shift the position of potential minimum and thus the conducting channel position in the lateral direction. Assuming the confinement has a conventional parabolic shape, we obtain that:

$$U(x) = \frac{m^* \omega^2 x^2}{2} + \alpha x = \frac{m^* \omega^2 (x - x_0)^2}{2},$$

where $x_0 = -\alpha/m^* \omega$ is the lateral shift. In this case in the experiment we would observe a smooth shift of the focusing peak as the ΔV_G changes. The case of double-well potential is qualitatively different because applying ΔV_G lowers one of the potential minima below the other one. At the same time the electron density relocates to the lower energy minimum (Fig. 3, *d*), i.e., the switching between two spatially separated conducting channels occurs. This shifting manifests itself in the experiment as the abrupt shift of the focusing peak. Besides the peak shift the doublet indicating the simultaneous filling of the both wells might have been expected. However, as seen from Fig. 3, *c*, this regime corresponds to the narrow range of ΔV_G values, which is impossible to analyze with the current accuracy.

Fig. 4, *a* describes a change of the focusing spectrum as the detector width changes by means of different sums of the gate voltages ΣV_G (the lower the ΔV_G is, the narrower the detector is) at $\Delta V_G = 0$. Each curve of the series corresponds to the different ΣV_G value that changed from -18 to -12 V. The measurement scheme is the same (see inset to Fig. 2). The peak height dependence on ΣV_G (Fig. 4, *b*) shows that widening the detector causes the focusing peak reduction. Indeed, the wider detector is, the more trajectories of ballistic electrons connect the injector and the detector, and a particular trajectory consequently becomes less resolvable.

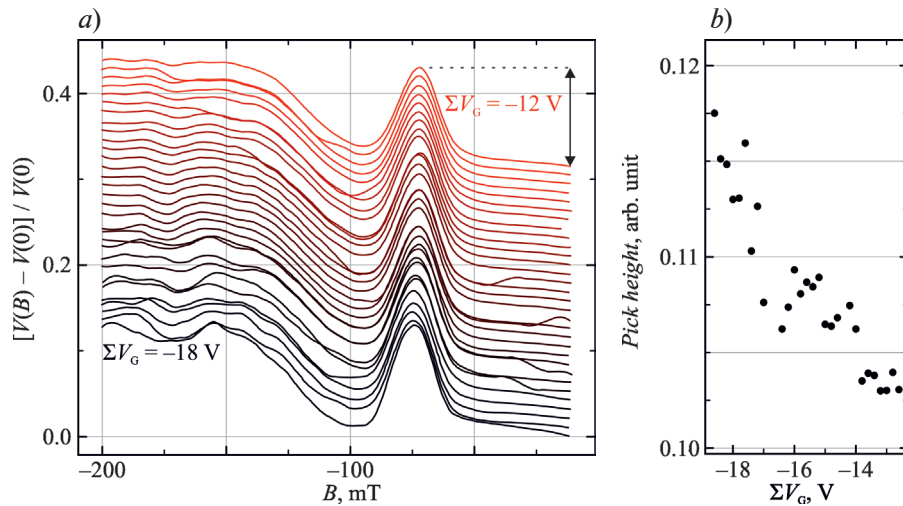


Fig. 4. Detector voltage dependence on the magnetic field at various detector ΣV_G values changing from -18 to -12 V (*a*). The lower curve corresponds to -18 V, and the upper curve to -12 V. The difference of gate voltages is zero. The measurement configuration is shown in the inset. The vertical arrow shows the focusing peak height. The focusing peak height as a function of the ΣV_G value (*b*)

Conclusion

We study the ballistic electron magnetotransport in the devices consisting of two similar trenched-type QPCs (injector and detector), located in the same plane and separated from each other at the distance of $4 \mu\text{m}$. The detector voltage demonstrates the peak at the magnetic field corresponding to the cyclotron diameter equal to the distance between the injector and the detector, caused by the magnetic focusing. Increasing the detector width by means of gate voltage is shown to lead to the focusing peak suppression. The best focusing peak observation condition is found to be $G_{\text{inj}} = G_{\text{det}} \sim 2e^2/h$. Applying the in-plane electric field by the injector gates asymmetrization causes the abrupt shift of the focusing peak by 2 mT . The corresponding cyclotron diameter change is about 100 nm , which is comparable with the characteristic distance between the conducting channels. The observed abrupt peak shift can be interpreted as the switching between two spatially separated conducting channels inside the QPC-injector.

REFERENCES

1. Wharam D.A., Thornton T.J., Newbury R., Pepper M., Ahmed H., Frost J.E.F., Hasko D.G., Peacock D.C., Ritchie D.A., Jones G.A.C., One dimensional transport and the quantisation of the ballistic resistance, *J. Phys. C: Solid State Phys.* 21 (1988) L209.
2. van Wees B.J., van Houten H., Beenakker C.W.J., Williamson J.G., Kouwenhoven L.P., van der Marel D., Foxon C.T., Quantized conductance of point contacts in a two-dimensional electron gas, *Phys. Rev. Lett.* 60 (1988) 848.
3. Masuda T., Sekine K., Nagase K., Wickramasinghe K.S., Mishima T.D., Santos M.B., Hirayama Y., Transport characteristics of InSb trench-type in-plane gate quantum point contact, *Appl. Phys. Lett.* 112 (2018) 192103.
4. Pokhabov D.A., Pogosov A.G., Zhdanov E.Yu., Bakarov A.K., Shklyayev A.A., Suspended quantum point contact with triple channel selectively driven by side gates, *Appl. Phys. Lett.* 115 (2019) 152101.
5. Pokhabov D.A., Pogosov A.G., Zhdanov E.Yu., Bakarov A.K., Shklyayev A.A., Double-Channel Electron Transport in Suspended Quantum Point Contacts with in-Plane Side Gates, *Semiconductors* 54 (2020) 1605.
6. Pokhabov D.A., Pogosov A.G., Zhdanov E.Yu., Bakarov A.K., Shklyayev A.A., Crossing and anticrossing of 1D subbands in a quantum point contact with in-plane side gates, *Appl. Phys. Lett.* 118 (2021) 012104.
7. Sarypov D.I., Pokhabov D.A., Pogosov A.G., Zhdanov E.Yu., Bakarov A.K., Multiwell Potential in a Trench-Type Quantum Point Contact, *JETP Lett.* 116 (2022) 360.
8. Pokhabov D.A., Pogosov A.G., Zhdanov E.Yu., Schevyrin A.A., Bakarov A.K., Shklyayev A. A., Lateral-electric-field-induced spin polarization in a suspended GaAs quantum point contact, *Appl. Phys. Lett.* 112 (2018) 082102.
9. Yakimenko I.I., Yakimenko I.P., Electronic properties of semiconductor quantum wires for shallow symmetric and asymmetric confinements, *J. Phys.: Condens. Matter* 34 (2022) 105302.
10. Zarenia M., Neilson D., Peeters F.M., Inhomogeneous phases in coupled electron-hole bilayer graphene sheets: Charge Density Waves and Coupled Wigner Crystals, *Sci. Rep.* 7 (2017) 11510.
11. Sharvin Yu.V., A Possible Method for Studying Fermi Surfaces, *Zh. Eksp. Teor. Fiz.* 48 (1965) 984.
12. Tsoi V.S., Focusing of electrons in a metal by a transverse magnetic field, *JETP Lett.* 19 (1974) 114.
13. Ho S.C., Chang H.J., Chang C.H., Lo S.T., Creeth G., Kumar S., Farrer I., Ritchie D.A., Griffiths J., Jones G., Pepper M., Chen T.M., Imaging the Zigzag Wigner Crystal in Confinement-Tunable Quantum Wires, *Phys. Rev. Lett.* 121 (2018) 106801.
14. Yan C., Kumar S., Thomas K., See P., Farrer I., Ritchie D.A., Griffiths J., Jones G., Pepper M., Engineering the spin polarization of one-dimensional electrons, *J. Phys.: Condens. Matter* 30 (2018) 08LT01.
15. Friedland K.-J., Hey R., Kostial H., Klann R., Ploog K., New Concept for the Reduction of Impurity Scattering in Remotely Doped GaAs Quantum Wells, *Phys. Rev. Lett.* 77 (1996) 4616.
16. Pogosov A.G., Budantsev M.V., Zhdanov E.Yu., Pokhabov D.A., Bakarov A.K., Toropov A. I., Electron transport in suspended semiconductor structures with two-dimensional electron gas, *Appl. Phys. Lett.* 100 (2012) 181902.
17. Pogosov A.G., Shevyrin A.A., Pokhabov D.A., Zhdanov E.Yu., Kumar S., Suspended semiconductor nanostructures: physics and technology, *J. Phys.: Condens. Matter* 34 (2022) 263001.
18. Lee Y.K., Smith J.S., Cole J. H., Influence of Device Geometry and Imperfections on the Interpretation of Transverse Magnetic Focusing Experiments, *Nanoscale Res Lett* 17 (2022) 31.



THE AUTHORS

SARYPOV Daniil I.

d.sarypov@g.nsu.ru

ORCID: 0000-0003-1056-5235

POKHABOV Dmitriy A.

pokhabov@isp.nsc.ru

ORCID: 0000-0002-8747-0261

POGOSOV Arthur G.

pogosov@isp.nsc.ru

ZHDANOV Evgeniy Yu.

zhdanov@isp.nsc.ru

BAKAROV Askhat K.

bakarov@isp.nsc.ru

ORCID: 0000-0002-0572-9648

Received 14.12.2022. Approved after reviewing 03.02.2023. Accepted 10.02.2023.